**Steel and Composite Structures**, *Vol. 31, No. 3 (2019) 319-327*
DOI: https://doi.org/10.12989/scs.2019.31.3.319


# Experimental study of the behavior of beam-column connections with expanded beam flanges

Hongwei Ma [*1], Jiwei Wang [2a], Eric M. Lui [3b], Zeqing Wan [1c] and Kun Wang [1d]

[1] *College of Civil Science and Engineering, Yangzhou University, Yangzhou, Jiangsu 225127, P.R. China*
[2] *College of Civil and Transportation Engineering, Hohai University, Nanjing, Jiangsu 210098, P.R. China*
[3] *Department of Civil & Environmental Engineering, Syracuse University, Syracuse, NY 13244, USA*

(*Received October 28, 2018, Revised March 20, 2019, Accepted April 24, 2019*)

**Abstract.** This paper describes an experimental study of steel beam-column connections with or without expanded beam flanges with different geometries. The objectives of this study are to elucidate the cyclic behavior of these connections, identify the location of the plastic hinge zone, and provide useful test data for future numerical simulations. Five connection specimens are designed and tested under cyclic load. The test setup consists of a beam and a column connected together by a connection with or without expanded beam flanges. A constant axial force is applied to the column and a time varying point load is applied to the free end of the beam, inducing shear and moment in the connection. Because the only effect to be studied in the present work is the expanded beam flange, the sizes of the beam and column as well as the magnitude of the axial force in the column are kept constant. However, the length, width and shape of the expanded beam flanges are varied. The responses of these connections in terms of their hysteretic behavior, failure modes, stiffness degradation and strain variations are experimentally obtained and discussed. The test results show that while the influence of the expanded beam flanges on hysteretic behavior, stiffness degradation and energy dissipation capacity of the connection is relatively minor, the size of the expanded beam flanges does affect the location of the plastic hinge zone and strain variations in these beam-column joints. Furthermore, in terms of ductility, moment and rotational capacities, all five connections behave well. No weld fracture or premature failure occurs before the formation of a plastic hinge in the beam.

**Keywords:** beam-column connections; expanded beam flanges; cyclic tests; hysteretic behavior; plastic hinge

## 1. Introduction

Moment frames derive their lateral load resisting capacity from the flexural and shear strengths of the framing members as well as from the rigidity and integrity of the beam-column connections. If the moment and shear demands at the connections are too high and if the connections are not properly designed, connection failure will occur. During the Northridge and Kobe earthquakes, numerous welded beam-column connections of steel moment frames experienced brittle fracture (White and Chen 1998, Miller 1998, Saher *et al*. 2017, Popov *et al*. 1998). To avoid similar connection failure occurring in future earthquakes, a number of innovative designs have been proposed. They can generally be classified as those that involve weakening the beam or strengthening the connection. Examples of the first group include reduced beam section (Wang *et al*. 2009, Pachoumis *et al*. 2009, 2010, Swati and Vesmawal 2014) as recommended by FEMA-350 (2000) and beam with perforated flanges (Rahnavard *et al*. 2015) or perforated web (Tsavdaridis *et al*. 2014, Tsavdaridis and Papadopoulos 2016). Examples of the second group include connections with steel fiber reinforced cementitious composites slabs (Cui *et al*. 2013), and connections with expanded beam flanges as shown in Fig. 1 (Wang *et al*. 2010, Zhang *et al*. 2011, Yang and Chen 2017) as recommended by the Chinese code (Ministry 2015).

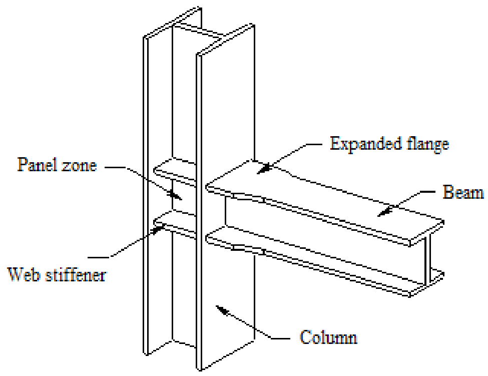

Fig. 1 A beam-column connection with expanded beam flanges

Although the main purpose of beam-column connections with reduced beam section and connections

∗Corresponding author, Ph.D.,
E-mail: hwma@yzu.edu.cn
[a] Professor, E-mail: wjw2903918@126.com
[b] Meredith Professor, E-mail: emlui@syr.edu
[c] Ph.D., E-mail: zqwan@yzu.edu.cn
[d] Ph.D., E-mail: wangkun@yzu.edu.cn


http://www.techno-press.org/?journal=scs&subpage=6
ISSN: 1229-9367 (Print), 1598-6233 (Online)

with expanded beam flanges is to relocate the plastic hinge away from the beam end so that plasticity occurs in the beam before cracking occurs in the welds. These connections also have different design intentions. The design intention for reduced beam section is to weaken the flanges or the web of the beams according to the seismic moment gradient so the section resistance moment gradient of the weakened region is more or less equal to the seismic moment demand gradient. The design intention for connections with expanded beam flanges (which is recommended by the Chinese code) is to provide a reinforced section in the beam according to the seismic moment gradient so the section resistance moment gradient of the reinforced area is greater than the seismic moment demand gradient. In either case, connection failure is avoided by ensuring that the moment resistance of the beam-column connection exceeds or at least equal to that of the demand.

Over the years, numerous studies on the effect reduced beam section has on steel beam-column connections have been carried out by Wang *et al*. (2009), Pachoumis *et al*. (2009, 2010), Sophianopoulos and Deri (2011), Han *et al*. (2012), Swati and Vesmawal (2014), and Oh *et al*. (2015). In comparison, relatively few studies on steel beam-column connections with expanded beam flanges have been performed (Lu *et al*. 2017, Wang *et al*. 2010, Zhang *et al*. 2011, Yang and Chen 2017, Chen and Lin 2013). In addition, these studies were primarily focused on the performance of the connections themselves without considering the effects different beam flange shapes and sizes may have on the cyclic behavior, plastic hinge location and failure modes of the connections. As a result, the main focus of the present study is to investigate the influence of flange shapes and sizes on the hysteretic behavior, moment and rotation capacities, plastic hinge location and failure modes of expanded beam flange connections.

To this end, five full-scale connection specimens were designed and fabricated. They were assembled and tested under cyclic loads in the structural laboratory of Nanjing Tech University. Of the five specimens, four have expanded beam flanges with different arc shapes, lengths and widths. They are used to study the influence these parameters may have on the behavior of the connection. The fifth is a control specimen without expanded beam flange to which the others can be compared.

In the following sections, detailed descriptions of the connection specimens, test setup, and test results will be provided. Based on these test results, the hysteretic behavior, moment capacity, ductility, plastic hinge location, energy dissipation capability, stiffness degradation, failure modes, and strain distributions on the flanges will be discussed.

## 2. Experimental program

### *2.1 Test specimens*

To investigate the influence of flange geometry and size on the behavior of connections with expanded beam flanges, five beam-column connection specimens were designed with the following variables: (1) with or without the presence of expanded flanges at beam end, (2) the expanded beam flanges take the shape of a convex or concave arc, and (3) different lengths and widths for the expanded beam flanges. These specimens were designated as S-1 to S-5 in Table 1. Both Specimens S-1 and S-2 have a concave arc (Fig. 2(a)) in the transition zone of the expanded beam flanges, but the flanges are of different sizes. The same set of flange sizes is used for Specimens S-3 and S-4, except that the flanges have a convex arc (Fig. 2(b)) in the transition zone. Specimen S-5 does not have expanded beam flanges and will serve as a control specimen. The effect of expanded beam flange sizes on connection behavior can be obtained by comparing the performance of Specimens S-1 with S-2, and that of S-3 with S-4. The effect of expanded beam flange shape on connection behavior can be obtained by comparing the performance of Specimens S-1 with S3, and that of S-2 with S-4. The effect of the presence of expanded beam flanges on connection behavior can be obtained by comparing the performance of Specimens S-1 to S-4 with Specimen S-5 (i.e., the control specimen).

All specimens were fabricated using Q235 steel with a nominal yield stress of 235 MPa. Coupon tests were conducted at Yangzhou University to determine the actual yield stress of the material. The results of six coupon tests showed that average yield stress was 287 MPa.

Table 1 Test specimens

| Specimen | Expanded flange parameters | | | |
|---|---|---|---|---|
| | $l_a$ (mm) | $l_b$ (mm) | $c$ (mm) | Arc shape |
| S-1 | 100 | 100 | 40 | Concave |
| S-2 | 200 | 200 | 50 | Concave |
| S-3 | 100 | 100 | 40 | Convex |
| S-4 | 200 | 200 | 50 | Convex |
| S-5 | N/A | N/A | N/A | N/A |

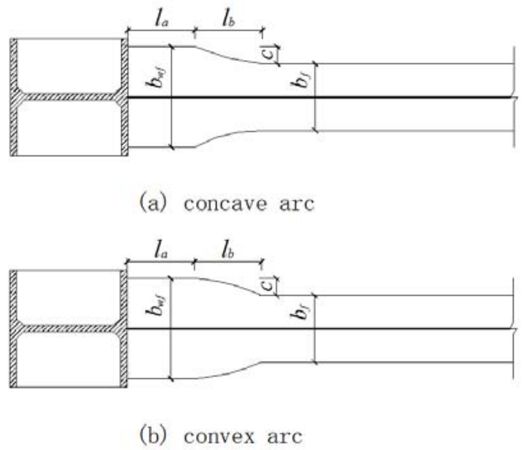


Fig. 2 Connections with expanded beam flanges

### *2.2 Test setup*

As shown in Fig. 3, the subassembly used for the connection tests consists of a cantilever beam welded to the flange of a column at mid-height using fillet welds. The electrode used was E4303 with a nominal weld strength of 421 MPa. The lengths of the beam and column are 1600 mm and 1800 mm, respectively. To allow for a direct comparison, the same beam and the same column sections were used for all five connection tests. The beam is HN400×200×8×12 and the column is HW350×350×12×12. In selecting the beam and column, the concept of "weak beam-strong column" (AISC 2018) was used in that plastic hinge was expected to form in the beam. The beam and column section dimensions and the calculated yield and plastic moments are given in Table 2. The specimens were fabricated by a local steel fabricator and all tests were performed in accordance with the Chinese code JGJ101/T-2015 (Ministry 2015). In the actual test, the entire test assembly was turned 90 degrees so the column was in a horizontal position and the beam was in a vertical position. A constant axial force was first applied to the column. A cyclic load was then applied to the free end of the beam at a distance of 1400 mm from the column face. A more detailed discussion of the load protocol will be given in Section 2.4.

To prevent local web yielding and web crippling, web stiffeners were provided in the panel zone of the column and at the free end of the cantilever beam as shown in Fig. 3. Furthermore, to prevent out-of-plane displacement, lateral braces were provided to the beam.

### *2.3 Test apparatus*

The test apparatus, which was used for all five tests, consists of: (1) A 500 kN hydraulic jack to apply an axial force to the column, (2) a 500 kN two-way hydraulic actuator to apply cyclic load to the beam, (3) a reaction wall to support the two-way hydraulic actuator, and (4) a strong floor to support the entire test assembly. As shown in Fig. 3, the instrumentation consists of: (1) two linear variable displacement transducers (LVDT) to determine the relative deformation of panel zone, (2) two LVDT to monitor the column displacement, (3) two LVDT to monitor the beam displacement, and (4) a load cell installed at one end of the column to measure the column axial force. In addition, strain gauges were placed on the beam flanges and on the expanded zone of the beam to determine strain changes as well as to monitor yielding in the expanded zone as shown in Fig. 4. The distances $l_1$, $l_2$, $l_3$, $l_4$, $l_5$, $l_6$ are set as follows: For Specimens S-1 and S-3, they are 30 mm, 35 mm, 35 mm, 33 mm, 33 mm, 34 mm, respectively; and for Specimens S-2, S-4 and S-5, they are 60 mm, 70 mm, 70 mm, 66 mm, 66 mm, 67 mm, respectively. All loads, displacements and strains were recorded in a data acquisition system at a rate of 50 channels per second. All recorded data were stored in a computer for subsequent analyses.

### *2.4 Loading protocol*

The loading protocol used for all five tests is as follows: A load equal to 500 kN was first applied to the column by a hydraulic jack. This load corresponds to about 20% of the yield load calculated based on the measured steel yield stress of 287 MPa. In the event that the strains recorded at all the measurement points on the column flanges were different, the load point was adjusted until the column was under uniform compression. This compressive axial force in the column was held constant for the entire duration of the test to simulate the actual loading conditions of a typical frame. In accordance with JGJ101-96 (Ministry 2015), a horizontal load which would induce a stress in the beam flanges equal to 30% of the material's yield strength was applied to the free end of the beam, and then fully unloaded to ensure that all the test equipment and instrumentations were performing properly and functioning as intended.

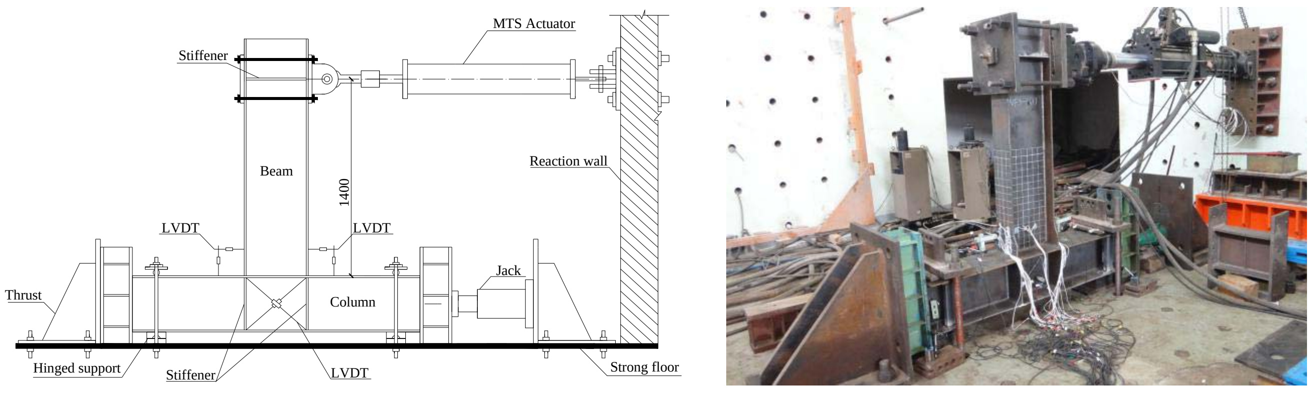


Fig. 3 Test setup

Table 2 Beam and column dimensions and calculated yield and plastic moments

| Member | Depth (mm) | Width (mm) | Flange thickness (mm) | Web thickness (mm) | Yield moment (kN·m) | Plastic moment (kN·m) |
|---|---|---|---|---|---|---|
| Beam | 400 | 200 | 12 | 8 | 290 | 396 |
| Column | 350 | 350 | 12 | 12 | 287 | 392 |

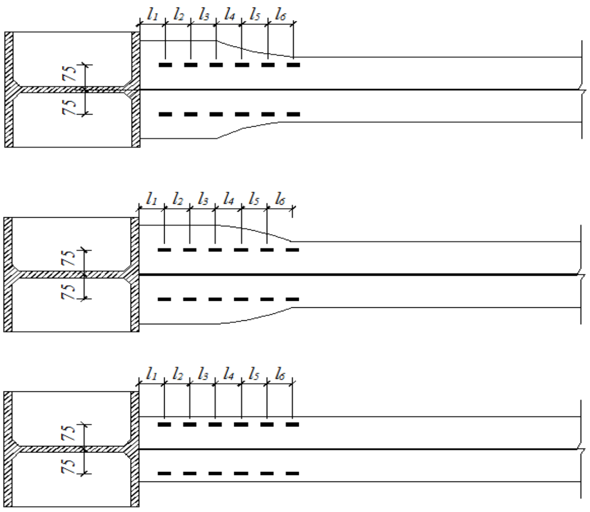


Fig. 4 Arrangement of measurement points (all dimensions in mm)

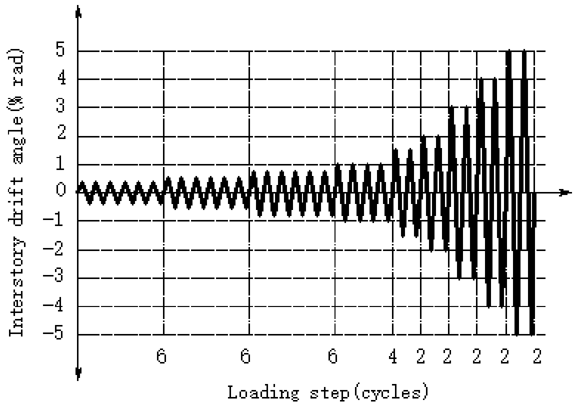


Fig. 5 Cyclic loading protocol

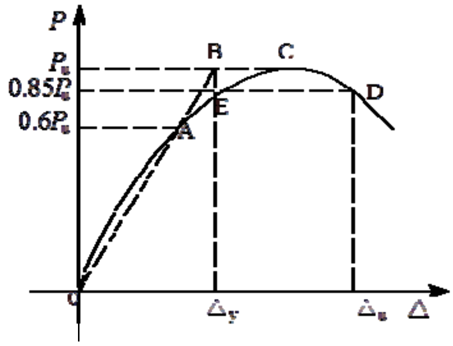


Fig. 6 Park's method to determine $\Delta_u$ and $\Delta_y$

A cyclic predetermined load sequence with gradually increasing displacement amplitudes as shown in Fig. 5 was then applied to the beam using the 500 kN two-way hydraulic actuator. The cyclic load history consists of six cycles of ±0.375%, ±0.5%, and ±0.75% rad story drifts, followed by four cycles of ±1% rad story drift and then with two cycles of ±1.5%, ±2%, ±3%, ±4%, and ±5% rad story drifts. Note that AISC (2018) defines special moment frame and intermediate moment frame systems as systems capable of providing an interstory drift of at least 4% and 2% rad, respectively. The displacement control load sequence continued to increase as multiples of the yield displacement, with three cycles at every displacement level until the specimen failed, or the load capacity fell to 85% of the maximum, or the maximum load capacity of the loading device was reached (FEMA-350 2000). The sign convention used is that a load applied in the leftward direction (i.e., when the arm of the hydraulic jack shown in Fig. 2 is extending) is considered positive.

## 3. Results and discussions

### 3.1 Test results

The test results for the maximum moment $M_{max}$, maximum drift angle $\theta_{max}$, ductility $\mu$, coefficient of energy dissipation $h_e$, and failure modes of the five specimens are summarized in Table 3. The maximum moment is the largest moment attained by the connection before it fails. It is obtained by multiplying the applied load by the distance measured from the point of application of the load to where the beam connects with the column. The maximum drift angle is calculated by dividing the maximum beam end deflection by the distance measured from the point of application of the load to the centerline of the column. The ductility is the ratio $\Delta_u/\Delta_y$, where $\Delta_u$ and $\Delta_y$ are determined using the Park's method (Park 1989) as illustrated in the load-deflection diagram in Fig. 6. The coefficient of energy dissipation (Wang *et al*. 2015, Guo *et al*. 2006) is defined as

$$h_e = \frac{S_{ABCD}}{S_{OAE} + S_{OCF}} \tag{1}$$

where, with reference to Fig. 7, $S_{ABCD}$ is the area enclosed by the last hysteretic loop before the specimen fails, and $S_{OAE}$ and $S_{OCF}$ are the areas of triangle OAE and triangle

Table 3 Summary of test results

| Specimen | $M_{max}$ (kN·m) | $\theta_{max}$ (rad) | $\mu$ | $h_e$ | Failure modes |
|---|---|---|---|---|---|
| S-1 | 395 | 0.0497 | 3.46 | 1.973 | Beam flange buckling / Plastic hinge formation |
| S-2 | 448 | 0.0498 | 3.22 | 2.055 | Beam flange buckling / Plastic hinge formation |
| S-3 | 420 | 0.0500 | 3.53 | 2.130 | Beam flange buckling / Plastic hinge formation |
| S-4 | 455 | 0.0499 | 3.45 | 2.293 | Beam flange buckling / Plastic hinge formation |
| S-5 | 434 | 0.0480 | 3.19 | 2.174 | Beam flange buckling / Plastic hinge formation |

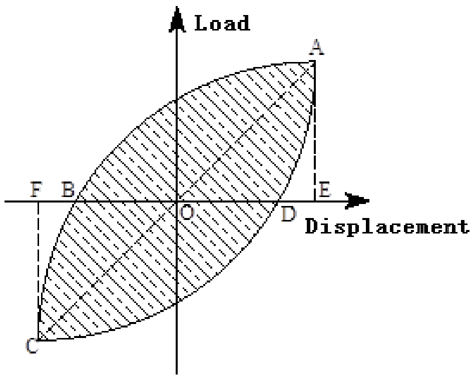


Fig. 7 Calculation of energy dissipation coefficient

OCF, respectively.

From Table 3, it can be seen that except for Specimens S-1 and S-3, all other specimens with expanded beam flanges have a higher moment capacity than Specimen S-5 (the control specimen), but all attained moments are equal to or larger than the nominal plastic moment capacity of the beam (which is equal to 396 kN-m). When compared to Specimen S-1, Specimen S-3 have slightly higher $M_{max}$, $\theta_{max}$, $\mu$ and $h_e$ values. The same can be said when one compares Specimen S-4 to Specimen S-2. This indicates that an expanded beam flange with a convex arc behaves slightly better than that with a concave arc. However, from a design perspective, this increase is not significant enough to be of much consequence.

All five specimens exhibit a ductility exceeding 3 and a coefficient of energy dissipation close to or larger than 2. These values are considered adequate for ordinary moment frame systems (ANSI/AISC 360-16); and since the assembly can withstand a drift angle of at least 4% radian without failure, the connections can potentially be used for intermediate and special moment frame systems as well (FEMA 350 2000, FEMA 351 2000). For all five specimens, the tests were terminated when plastic hinge formed in the beam. However, the location of plastic hinge zone is different for the specimens. This will be discussed in more detail in a later section.

### *3.2 Hysteretic behavior*

The load-deflection hysteretic curves obtained for the five specimens are presented in Fig. 8. From these figures, it is observed that:

- The hysteretic loops for all five specimens are plump. No cracks were observed at the welds of all the specimens during the entire test protocol. The test results indicate that all the connection specimens have good ductility and energy dissipation capability.
- Upon comparison with the control specimen (S-5), the specimens with expanded beam flanges (S-1 to S-4) exhibit a slight pinching effect at load cycles that correspond to high drift angles (Fig. 5). This is due to an earlier initiation of local flange buckling given that the width-thickness ratio of the expanded beam flanges are higher for Specimens S-1 to S-4.
- When compared with Specimen S-1, the hysteretic loop of Specimen S-2 shows that it has a higher load capacity and an increased energy dissipation capability. The same observation applies to

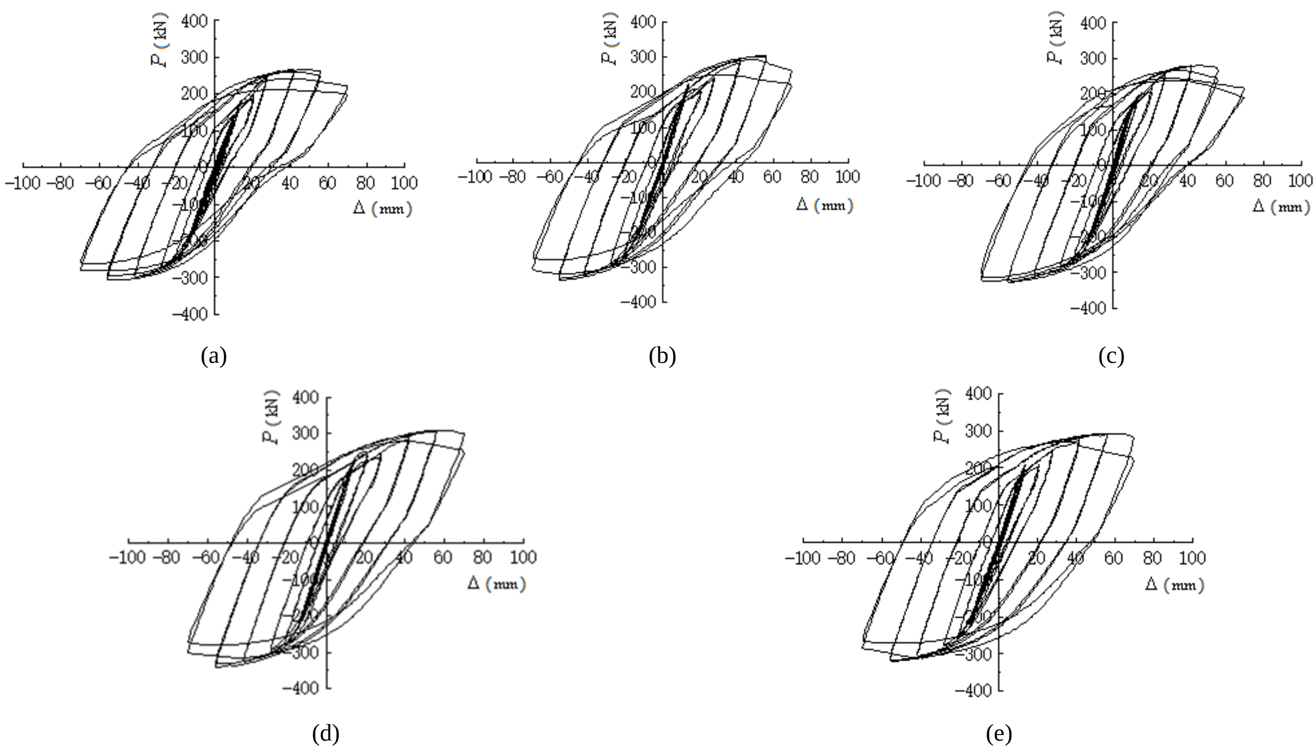


Fig. 8 Hysteretic curves of test specimens: (a) S-1; (b) S-2; (c) S-3; (d) S-4; (e) S-5

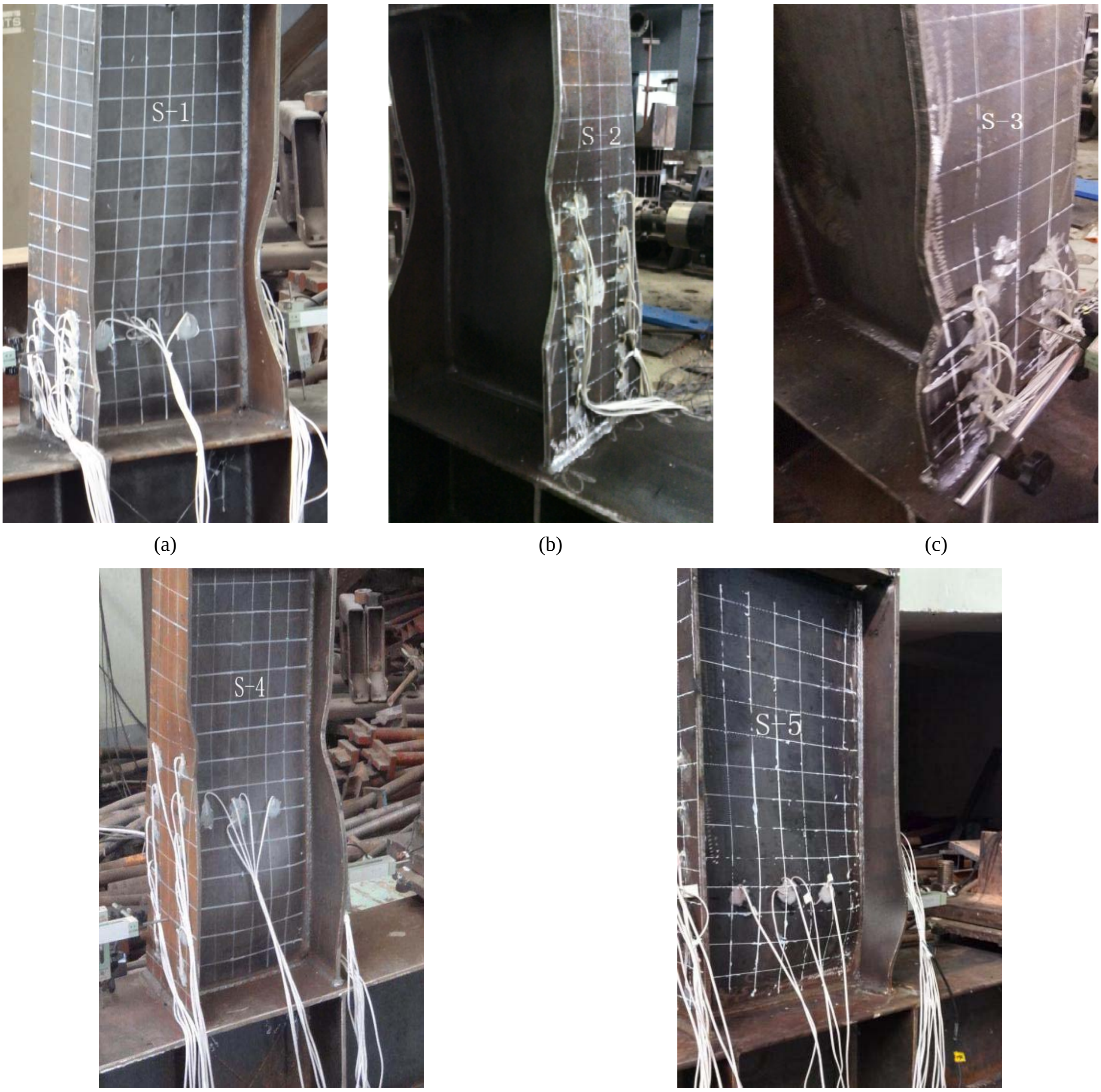


(a) (b) (c)

(d) (e)

Fig. 9 Specimens S-1, S-2, S-3, S-4 and S-5 at $\theta = 5\%$ rad

Specimen S-4 when compared to Specimen S-3. These results are expected since the expanded beam flanges of Specimens S-2 and S-4 are larger than those of Specimens S-1 and S-3, respectively.

### *3.3 Experimental observations*

When the drift angle $\theta$ was between 0.375% and 1% rad, all members of the test assembly deformed elastically. When $\theta$ reached 2% rad, the beam flanges of all specimens began to experience local buckling. When measured from the beam end, this flange buckling occurred at a distance of 150 mm, 450 mm, 150 mm, 450 mm, and 70 mm for Specimens S-1 to S-5, respectively. When $\theta$ approached 3% rad, the zone between 100 mm to 350 mm for Specimen S-1, between 400 mm to 550 mm for Specimen S-2, between 100 mm to 350 mm for Specimen S-3, between 400 mm to 550 mm for Specimen S-4, and between 50 mm to 200 mm for Specimen S-5 began to experience inelastic deformation and signified the zone where a plastic hinge would form. When $\theta$ reached 4% rad, out-of-plane deformation was observed for the beam web for all specimens, but the deformation was rather small for Specimen S-5. The maximum load for all five specimens was reached when $\theta$ was approximately equal to 5% rad (Fig. 9). From this point on, the load started to decrease when a plastic hinge was formed in the beam.

Although the hysteretic loops of Specimen S-5 do not exhibit any pinching effect at all load levels during the test, the location of the plastic hinge zone for this specimen is

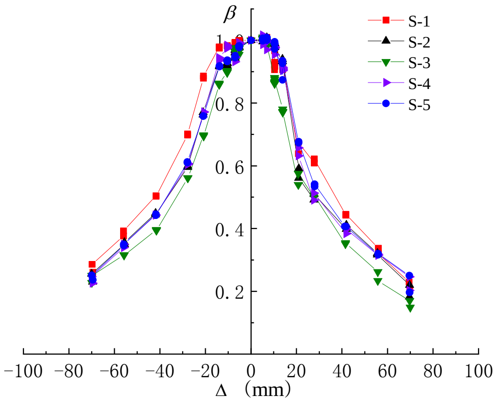


Fig. 10 Variation of stiffness with drift

quite close to the beam end, which is considered undesirable. In comparison, the plastic hinge zone for all specimens with expanded beam flanges is further away from the beam end, with Specimen S-2 or S-4 being the farthest.

### *3.4 Stiffness degradation coefficient*

With reference to Fig. 10, when the drift angle is in the range of 0.375% to 1% rad (which corresponds to a drift Δ of approximately 6 mm to 16 mm), the stiffness $\beta$ of all specimens does not vary significantly, indicating that the deformation is elastic.

Herein, $\beta$ is defined as

$$\beta = \frac{\sum_{i}^{n} P_i}{\sum_{i}^{n} \Delta_i} \tag{2}$$

where $P_i$ and $\Delta_i$ are the peak load and peak displacement in the $i$-th load cycle, respectively.

When $\theta$ is between 0.375% and 1% rad, the stiffness of the five specimens shows no degradation. Degradation of stiffness occurs rather rapidly when $\theta$ exceeds 1% rad (i.e., when Δ exceeds ≈16 mm). As Δ increases, the degradation rate decreases. For a given Δ, $\beta$ appears to be the highest for Specimen S-1 and lowest for Specimen S-3, with the others in between and being quite comparable to one another.

### *3.5 Longitudinal strain variations along beam flange*

Figs. 11(a)-(e) show how the measured longitudinal strain ε varies along the beam flange zone for the five specimens. In the figures, D is the distance measured from the face of the column. For a given D, longitudinal strains are plotted for eight displacement values (Δ = 7, 10.5, 14.0, 21.0, 28.0, 42.0, 56.0, 70.0 mm). From the figures, it can be seen that ε generally increases as Δ increases. However, the increase is not linear. The increase in ε is quite small for small Δ, but it becomes more prominent when Δ gets larger, signifying that the connection is behaving nonlinearly. Also, when Δ is small (≤ 14 mm), the variation of ε with D is relatively small. However, large changes in ε occurs when Δ gets larger (≥ 21 mm). Since the yield strain was calculated to be around $1400\times10^{-6}$, any strain that exceeds this value means yielding of the flange has occurred. Once yielding has occurred, the variation of ε with D does not follow a specific pattern. This is because in addition to the complex geometries of the expanded flanges used in the present study (Fig. 2), the effect of residual stresses and plastic hinge formation start to play a role in affecting the strain distributions.

When one compares the strains for the specimens, it can

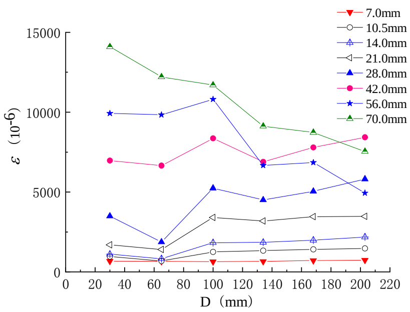


(a) S-1

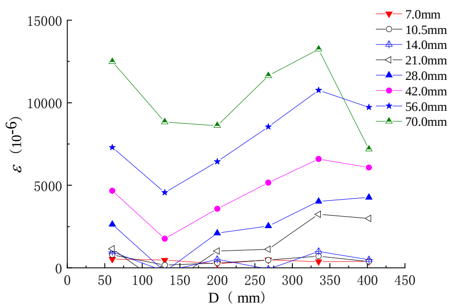


(b) S-2

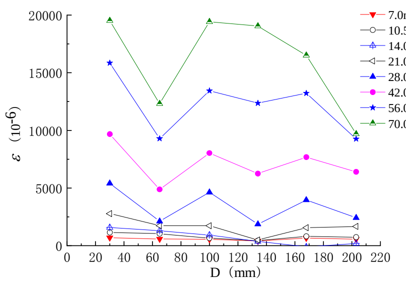


(c) S-3

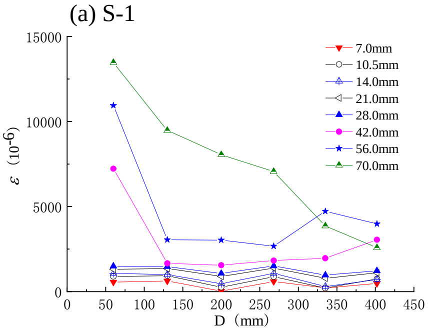


(d) S-4

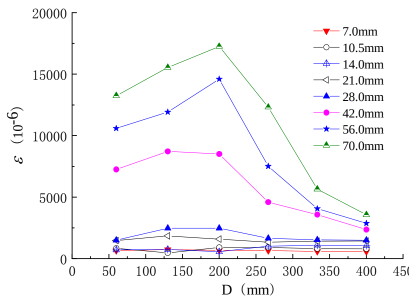


(e) S-5

Fig. 11 Longitudinal strains on beam flange for Specimen be seen that for a given Δ, $\varepsilon$ for Specimen S-1 in the range $0 \leq D \leq 200$ mm are generally higher than those of Specimen S-2, and $\varepsilon$ for Specimen S-3 in the range $0 \leq D \leq 200$ mm are generally higher than those of Specimen S-4, with Specimen S-5 somewhere in between. The higher strain can be attributed to the shorter length of the expanded beam flanges for Specimen S-1 and S-3. Moreover, for the same range of D, ε for Specimen S-1 are generally lower than those of Specimen S-3, and $\varepsilon$ for Specimen S-2 are generally lower than those of Specimen S-4. This means for the same expanded beam flange length, the shape (concave vs. convex) of the beam flange in the transition zone can have an effect on strain distribution.

## 4. Conclusions

In this paper, an experimental study of five full scale moment resisting connections is presented. Of the five test specimens, four have expanded beam flanges and the one without expanded beam flanges was used as a control. The parameters to be investigated were the length, width and shape of the expanded beam flanges. For a given length and width, two specimens: one with a concave arc and another with a convex arc in the transition zone of the beam flanges were fabricated, tested and compared. The connections were tested in a subassembly consisted of a beam with the connection at one end welded to the mid-height of a column. A constant axial force was applied to the column, while a cyclic point load was applied to the free end of the beam. The performance of the connections in terms of their hysteretic behavior, moment capacity, ductility, energy dissipation capability, stiffness degradation, failure modes, and strain distributions on the flanges was discussed. From these tests, the following observations can be made:

- The hysteretic curves for all five specimens are relatively stable, the curves of S-1, S-2, S-3 and S-4 exhibit slight pinching, and the moment capacities of S-2 and S-4 are higher than those of the other three specimens.
- All connections are able to develop the nominal plastic moment capacity of the beam without weld fracture.
- Although all connections failed by formation of plastic hinge in the beam after local buckling of the beam flanges was observed, the location of the plastic hinge zone is different. For Specimens S-2 and S-4, the zone of plastic deformation is further away from beam end.
- From the measured longitudinal strains ε along the beam flanges for specimens with the same expanded beam flange length, the geometry of the beam flange in the transition zone can have an effect on the strain distributions.
- Although the connections with larger expanded beam flanges have higher moment capacities and coefficients of energy dissipation, and smaller flange strains, they are not considered to be of significance for purpose of design.
- When compared to connections with concave arc in the beam flanges, connections with convex arc have slightly higher moment and rotation capacities, ductility and coefficients of energy dissipation. However, the increase is quite small and can therefore be ignored.

The major advantage of using connections with expanded beam flanges is to move the location of plastic hinge away from the column face. For Specimen S-5 (the control specimen without the expanded beam flanges), the plastic hinge zone is 50 mm - 200 mm from the column face. For Specimen S-1 and S-3 (the specimens with the shorter and narrower expanded beam flanges), the plastic hinge zone is 100 mm - 350 mm from the column face, and for Specimen S-2 and S-4 (the specimens with the longer and wider expanded beam flanges), the plastic hinge zone is 400 mm - 550 mm from the column face.

## Acknowledgments

The authors appreciate the support of the National Science Foundation of China (51878589 and 51878590), the Production and Research Foundation of Jiangsu Province (BY2016069-01), the Science and Technology projects of Ministry of Housing and Urban-rural Development (2014-K2-045 and 2014-K2-022), the Talent Plan of Innovate and Entrepreneurship in Jiangsu Province and the Talent Plan of Yangzhou City. The writers are also grateful to the reviewers for their useful comments and suggestions.

## References

AISC (2018), Seismic Design Manual; (3rd edition), American Institute of Steel Construction, Chicago, IL, USA.

ANSI/AISC 360-16 (2016), Specification for Structural Steel Buildings; American Institute of Steel Construction, Chicago, IL, USA.

Chen, C.C. and Lin, C.C. (2013), "Seismic performance of steel beam-to-column moment connections with tapered beam flanges", *Eng. Struct.*, **48**, 588-601.

Cui, Y., Luo, Y.B. and Nakashima, M. (2013), "Development of steel beam-to-column connections using SFRCC slabs", *Eng. Struct.*, **52**, 545-557.

FEMA-350 (2000), Recommended Seismic Design Criteria for New Steel Moment-Frame Buildings; Federal Emergency Management Agency, Sacramento, CA, USA.

FEMA-351 (2000), Recommended Seismic Evaluation and Upgrade Criteria for Existing Welded Steel Moment-Frame Buildings; Federal Emergency Management Agency, Sacramento, CA, USA.

Guo, B., Gu, Q. and Liu, F. (2006), "Experimental behavior of stiffened and unstiffened end-plate connections under cyclic loading", *J. Struct Eng.*, **132**, 1352-1357.

Han, S.W., Moon, K.H., Hwang, S.H. and Stojadinovic, B. (2012), "Rotation capacities of reduced beam section with bolted web (RBS-B) connections", *J. Constr Steel Res.*, **70**, 256-263.

Lu, L.F., Wang, L.L., Xu, Y.L. and Zhang, H.S. (2017), "Finite element analysis on hysteretic behavior of joint with side-plate reinforced beam flange weak-axis connection of steel frames",

*J. Xi'an Univ. Arch. Tech.*, **49**(5), 646-653. [In Chinese]
Miller, D.K. (1998), "Lessons learned from the Northridge earthquake", *Eng. Struct*, **20**(4-6), 249-260.
Ministry of Housing and Urban-Rural Development of the People's Republic of China (2015), Specification of Testing Methods for Earthquake Resistant Building; Architecture & Building Press, Beijing, China. [In Chinese]
Oh, K.Y., Lee, K.M., Chen, L.Y., Hong, S.B. and Yang, Y. (2015), "Seismic performance evaluation of weak axis column-tree moment connections with reduced beam section", *J. Constr. Steel Res.*, **105**, 28-38.
Pachoumis, D.T, Galoussis, E.G., Kalfas, C.N. and Christitsas, A.D. (2009), "Reduced beam section moment connections subjected to cyclic loading: Experimental analysis and FEM simulation", *Eng. Struct.*, **31**(1), 216-223
Pachoumis, D.T., Galoussis, E.G., Kalfas, C.N. and Efthimiou, I.Z. (2010), "Cyclic performance of steel moment-resisting connections with reduced beam sections - experimental analysis and finite element model simulation", *Eng. Struct.*, **32**, 2683-2692.
Park, R. (1989), "Evaluation of ductility of structures and structural subassemblages from laboratory testing", *Bull. New Zealand Soc. Earthq. Eng.*, **22**(3), 155-166.
Popov, E.P., Yang, T.S. and Chang, S.P. (1998), "Design of steel MRF connections before and after 1994 Northridge earthquake", *Eng. Struct.*, **20**(12), 1030-1038.
Rahnavard, R., Hassanipour, A. and Siahpolo, N. (2015), "Analytical study on new types of reduced beam section moment connections affecting cyclic behavior", *Case Studies in Struct. Eng.*, **3**, 33-51.
Saher, E.K., Sakr, M.A., Khalifa, T.M. and Eladly, M.M. (2017), "Modelling and behavior of beam-to-column connections under axial force and cyclic bending", *J. Constr. Steel Res.*, **129**, 171-184.
Sophianopoulos, D.S. and Deri, A.E. (2011), "Parameters affecting response and design of steel moment frame reduced beam section connections: An overview", *Int. J. Steel Struct.*, **11**(2), 133-144.
Swati, A.K. and Vesmawal, G. (2014), "Study of steel moment connection with and without reduced beam section", *Case Studies in Eng. Struct.*, **1**, 26-31.
Tsavdaridis, K.D. and Papadopoulos, T. (2016), "A FE parametric study of RWS beam-to-column bolted connections with cellular beams", *J. Constr. Steel Res.*, **116**, 92-113.
Tsavdaridis, K.D., Faghih, F. and Nikitas, N. (2014), "Assessment of perforated steel beam-to-column connections subjected to cyclic loading", *J. Earthq. Eng.*, **18**, 1302-1325.
Wang, W.Z., Xiang, F. and Xu, J.X. (2009), "Effective length factor of column in sway steel frames with dog-bone connections", *J. Xi'an Univ. Arch. Tech.*, **41**(6), 775-779. [In Chinese]
Wang, Y., Gao, P., Yu, Y.S. and Wang, Y.T. (2010), "Experimental study on beam-to-column connections with beam-end horizontal haunch of steel frame under low cyclic loading", *J. Build. Struct.*, **31**(4), 94-101. [In Chinese]
Wang, Q.W., Shi, Q.X. and Tian, H.H. (2015), "Seismic behavior of steel reinforced concrete (SRC) joints with new-type section steel under cyclic loading", *Steel Compos. Struct., Int. J.*, **19**(6), 1561-1580.
White, D.W. and Chen, W.F. (1998), "Organization and summary of discussions at the US-Japan seminar on innovations in stability concepts and methods for seismic design in structural steel", *Eng. Struct.*, **20**(4-6), 242-248.
Yang, L. and Chen, H. (2017), "Mechanical performance of beam-column joint with widened beam flange", *J. Shenyang Univ. Tech.*, **39**(4), 459-463. [In Chinese]
Zhang, W.Y., Wang, X.J., Zhu, F.J. and Zhang, Y.C. (2011), "Seismic behavior and design method of beam-to-column connections with beam-end horizontal haunches", *J. Harbin Inst. Tech.*, **41**(12), 7-13. [In Chinese]

*CC*